

An Empirical UBVRIJHK Temperature Calibration for Stars

Guy Worthey and Hyun-chul Lee

Department of Physics and Astronomy, Washington State University, Pullman, WA 99164-2814

ABSTRACT

A collection of Johnson/Cousins photometry for stars with known [Fe/H] is used to generate color-color relations that include abundance and gravity dependences. Literature temperatures and bolometric corrections are attached to make an empirical transformation table. Unlike synthetic colors, the empirical ones generally show about the same gravity dependence at different metallicities, and about the same metallicity dependence at different gravities.

1. The Color-Color Relations

This short talk extends a paper that is being refereed at the present moment concerning an empirical color-temperature relation that tabulates colors as a function of stellar $\log g$, [Fe/H], and effective temperature. About 3000 stars with literature abundance estimates and multicolor photometry were collected. The final table and accompanying interpolation program are available at <http://astro.wsu.edu/models/>.

Figures one through six display various colors versus $V - K$, a good temperature indicator for cool stars. Except for $H - K$, marked gravity dependences can be noted in the figures, but redder colors are all fairly insensitive to abundance variations at the few-percent level. Fits are also shown in the figures. Supergiants are included in all fits, but carbon stars were not considered at all.

Figures 7 and 8 show some of the temperature calibrations that were considered for attachment to the color-color tables at the cool end. Not shown are the hot star temperatures

and the bolometric corrections that were also attached.

2. Comparison with Synthetically Produced Colors

Figures 9 through 12 show color partial derivatives as a function of abundance, plotted versus temperature for two values of $\log g$. Except for the ends of the temperature range plotted, the empirical relation should be accurate to a few hundredths of a magnitude. However, when comparing synthetic colors versus the empirical ones, excursions of 0.3 mag (= 0.15 mag per factor of ten in abundance) are seen in most of these diagrams.

Figures 13 through 16 show analogous color responses, but this time with respect to gravity. Large excursions are also seen in this dimension, substantially larger than plausible empirical errors. The fact that the gravity excursions are so large may indicate that atmosphere structures are drifting from reality (not just that the line lists are immature).

Of note in all of the derivative figures (9 through 16) is the close agreement of the bi-

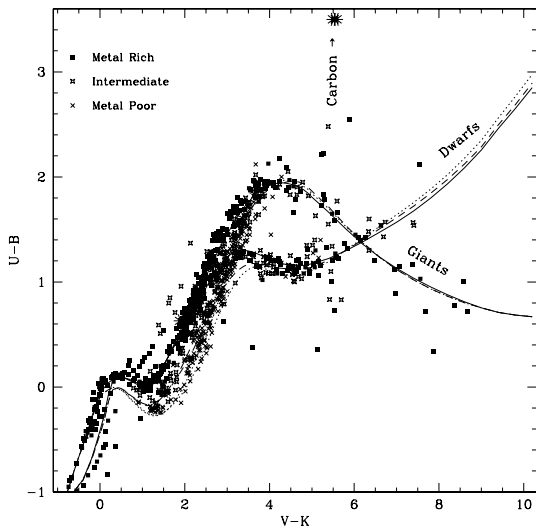


Fig. 1.— The $U - B$, $V - K$ color-color diagram for uncultured stars. Stars have different symbol types for metal rich ($[\text{Fe}/\text{H}] > -0.2$), metal-poor ($[\text{Fe}/\text{H}] < -1.2$), and intermediate abundance ranges. Calibrations for typical giant and typical dwarf gravities are drawn in solid for $[\text{Fe}/\text{H}] = 0$, dashed for $[\text{Fe}/\text{H}] = -1$, and dotted for $[\text{Fe}/\text{H}] = -2$. Most carbon stars (asterisks) are not plotted as they stretch beyond the plot limits along a line from the plotted ones up to $(V - K, U - B) \approx (6, 6)$.

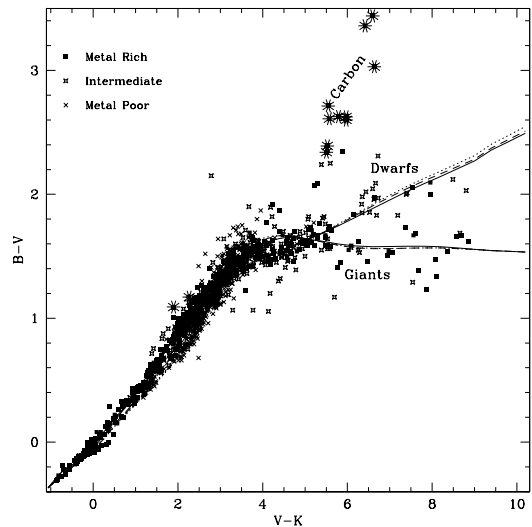


Fig. 2.— The $B - V$, $V - K$ color-color diagram for uncultured stars. Stars have different symbol types for metal rich ($[\text{Fe}/\text{H}] > -0.2$), metal-poor ($[\text{Fe}/\text{H}] < -1.2$), and intermediate abundance ranges. Calibrations for typical giant and typical dwarf gravities are drawn in solid for $[\text{Fe}/\text{H}] = 0$, dashed for $[\text{Fe}/\text{H}] = -1$, and dotted for $[\text{Fe}/\text{H}] = -2$. Carbon stars are shown as asterisks.

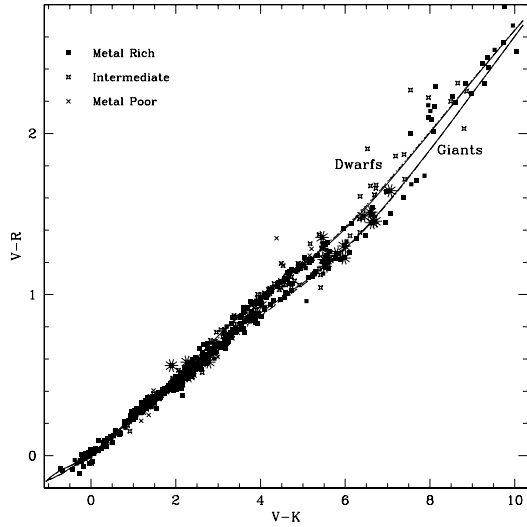


Fig. 3.— The $V - R$, $V - K$ color-color diagram for uncultured stars. Symbols and line styles are as in Figure 2.

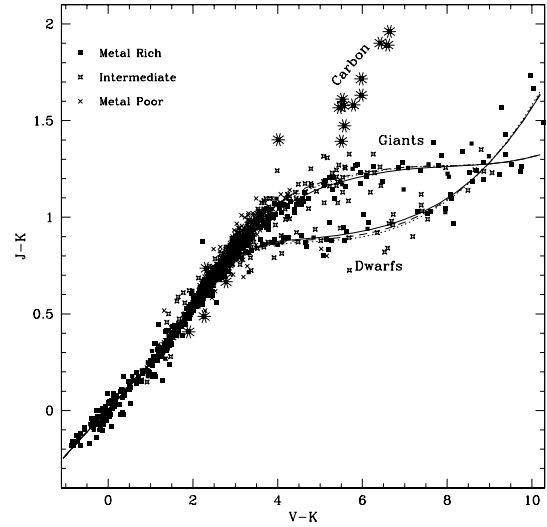


Fig. 5.— The $J - K$, $V - K$ color-color diagram for uncultured stars. Symbols and line styles are as in Figure 2.

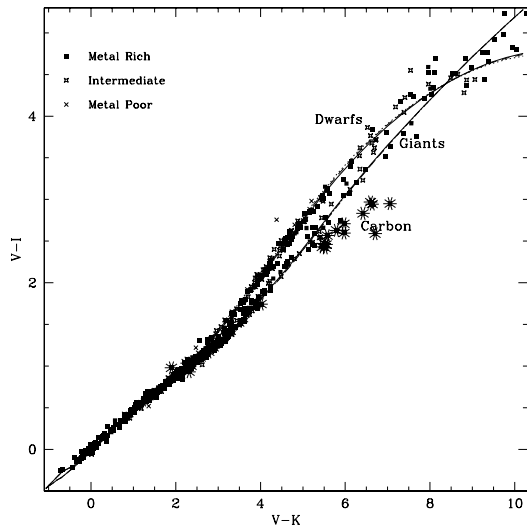


Fig. 4.— The $V - I$, $V - K$ color-color diagram for uncultured stars. Symbols and line styles are as in Figure 2.

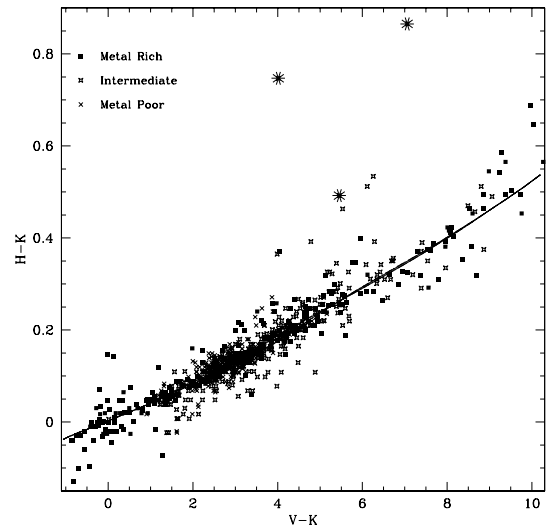


Fig. 6.— The $H - K$, $V - K$ color-color diagram for uncultured stars. Symbols and line styles are as in Figure 2.

colored lines. This indicates that the metallicity sensitivity is about the same at different gravities (Figs 9-12) and that the gravity sensitivity is about the same for stars of different abundances (Figs 13-16). The fitting functions were flexible enough to capture any variations, so this appears to be a real feature of real stars.

Major funding for this work was provided by the National Science Foundation grant AST-0307487, the New Standard Stellar Population Models project. GW would like to thank the undergraduates who have typed in data pertaining to stars over the more than 11 years this empirical color project has stretched. Brent Fisher (Worthey & Fisher 1996) and Joey Wroten at the University of Michigan and Jared Lohr and Ben Norman at Washington State University.

REFERENCES

- Alonso, A., Arribas, S., & Martinez-Roger, C. 1999, *A&AS*, 139, 335
- Alonso, A., Arribas, S., & Martinez-Roger, C. 1999, *A&AS*, 140, 261
- Basri, G., Mohanty, S., Allard, F., Hauschildt, P. H., Delfosse, X., Martín, E. L., Forveille, T., & Goldman, B. 2000, *ApJ*, 538, 363
- Berger, D. H., Gies, D. R., McAlister, H. A., ten Brummelaar, T. A., Henry, T. J., Strurmann, J., Sturmann, L., Turner, N. H., Ridgway, S. T., Aufdenberg, J. P., & Mérand, A. 2006, *astro-ph/0602105*
- Berriman, G., Reid, N., & Leggett, S. K. 1992, *ApJ*, 392, L31
- Bessell, M. S., Castelli, F., & Plez, B. 1998, *A&A*, 333, 231, erratum 1998, *A&A*, 337, 321
- Dawson, P. C., & De Robertis, M. M. 2004, *AJ*, 127, 2909
- Johnson, H. L. 1966, *ARA&A*, 4, 193
- Tokunaga, A. T. 2000, in *Astrophysical Quantities*, 4th ed., ed. A. N. Cox, p. 143
- Torres, G., & Ribas, I. 2002, *ApJ*, 567, 1140
- VandenBerg, D. A., & Clem, J. L. 2003, *AJ*, 126, 778
- Viti, S., Jones, H. R. A., Schweitzer, A., Allard, F., Hauschildt, P. H., Tennyson, J., Miller, S., & Longmore, A. J. 1997, *MNRAS*, 291, 780
- Worthey, G. 1994, *ApJS*, 95, 107
- Worthey, G., & Fisher, B. 1996, *BAAS*, 189, 72.05
- Yi, S., Demarque, P., Kim, Y.-C., Lee, Y.-W., Ree, C. H., Lejeune, T., & Barnes, S. 2001, *ApJS*, 136, 417

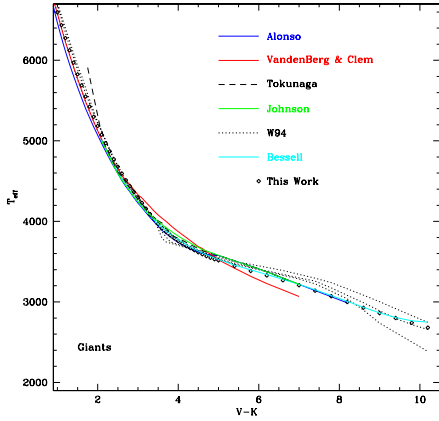


Fig. 7.— Temperature- $V - K$ calibrations for cool, solar abundance giants. Lines are color-coded for the calibrations of Alonso et al. (1999a,b); Vandenberg & Clem (2003); Tokunaga (2000); Johnson (1966); Worthey (1994); Bessell et al. (1998). Our adopted relation is shown as diamonds.

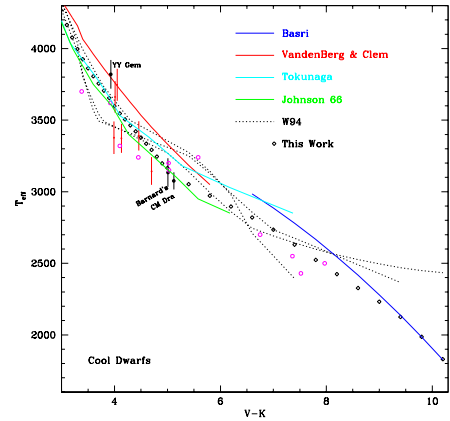


Fig. 8.— Temperature- $V - K$ calibrations for cool, solar abundance dwarfs. Lines are color-coded for the calibrations of Vandenberg & Clem (2003); Tokunaga (2000); Johnson (1966); Worthey (1994); Bessell et al. (1998) and Baeri et al. (2000). Red dots with error bars are M dwarfs from Berger et al. (2006) and magenta open circles are TIRFM temperatures and photometry from Berriman et al. (1992). YY Geminorum's temperature is from Torres & Ribas (2002), Barnard's star from Dawson & de Robertis (2004), and CM Draconis's from Viti et al. (1997). The adopted empirical relation is shown as diamonds.

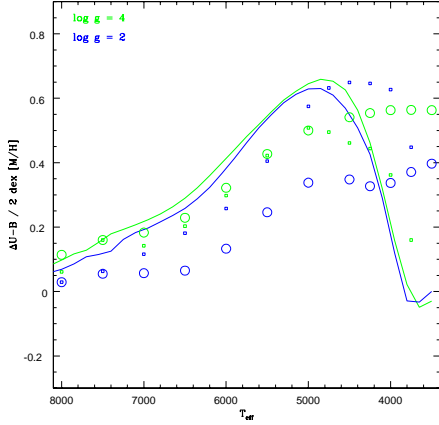


Fig. 9.— The change in $U - B$ color caused by a shift in $[\text{Fe}/\text{H}]$ from -2 to 0 is shown as a function of effective temperature. The empirical relation is shown as lines, the Kurucz colors used by Worthey (1994) are small squares, and the color table attached to the YY isochrones (Yi et al. 2001) are shown as large open circles. Results for two gravity regimes are shown.

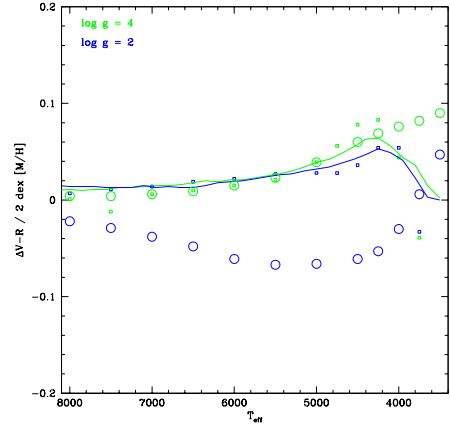


Fig. 11.— The change in $V - R$ color caused by a shift in $[\text{Fe}/\text{H}]$ from -2 to 0 is shown as a function of effective temperature. Symbols as in Fig. 9.

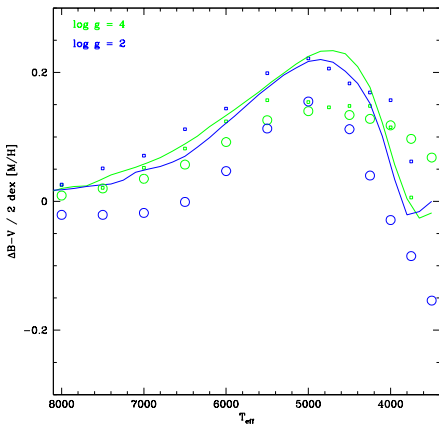


Fig. 10.— The change in $B - V$ color caused by a shift in $[\text{Fe}/\text{H}]$ from -2 to 0 is shown as a function of effective temperature. Symbols as in Fig. 9.

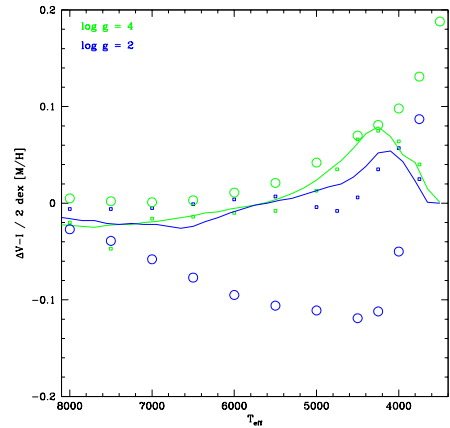


Fig. 12.— The change in $V - I$ color caused by a shift in $[\text{Fe}/\text{H}]$ from -2 to 0 is shown as a function of effective temperature. Symbols as in Fig. 9.

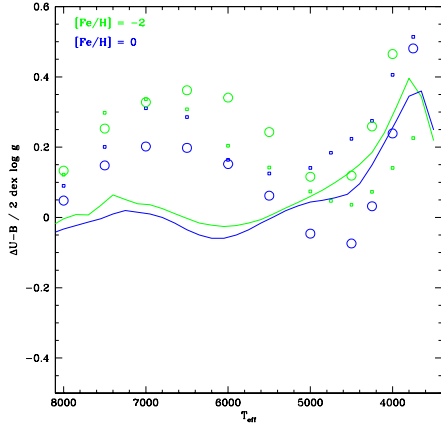


Fig. 13.— The change in $U - B$ color caused by a shift in $\log g$ from 2 to 4 is shown as a function of effective temperature. The empirical relation is shown as lines, the Kurucz colors used by Worthey (1994) are small squares, and the color table attached to the YY isochrones (Yi et al. 2001) are shown as large open circles. Results for two metallicity regimes are shown.

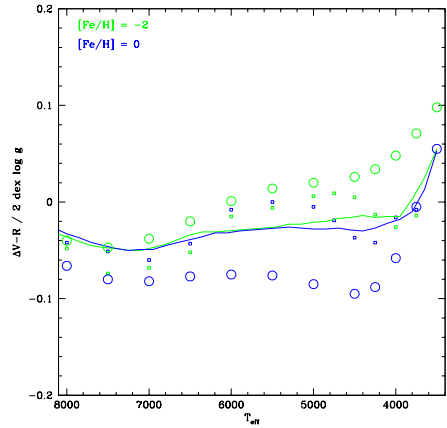


Fig. 15.— The change in $V - R$ color caused by a shift in $\log g$ from 2 to 4 is shown as a function of effective temperature. Symbols as in Fig. 13.

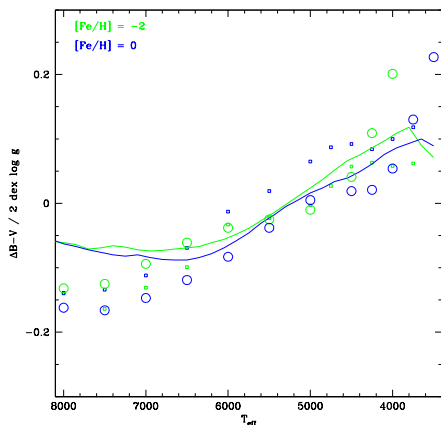


Fig. 14.— The change in $B - V$ color caused by a shift in $\log g$ from 2 to 4 is shown as a function of effective temperature. Symbols as in Fig. 13.

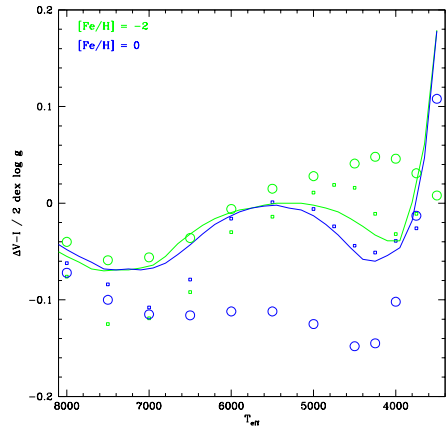


Fig. 16.— The change in $V - I$ color caused by a shift in $\log g$ from 2 to 4 is shown as a function of effective temperature. Symbols as in Fig. 13.